

RESEARCH ARTICLE

Open Access



Effects of capecitabine treatment on the uptake of thymidine analogs using exploratory PET imaging agents: ^{18}F -FAU, ^{18}F -FMAU, and ^{18}F -FLT

Christopher I. McHugh¹, Jawana M. Lawhorn-Crews², Dipenkumar Modi², Kirk A. Douglas², Steven K. Jones¹, Thomas J. Mangner³, Jerry M. Collins⁴ and Anthony F. Shields^{2*}

Abstract

Background: A principal goal for the use of positron emission tomography (PET) in oncology is for real-time evaluation of tumor response to chemotherapy. Given that many contemporary anti-neoplastic agents function by impairing cellular proliferation, it is of interest to develop imaging modalities to monitor these pathways. Here we examined the effect of capecitabine on the uptake of thymidine analogs used with PET: 3'-deoxy-3'-[^{18}F]fluorothymidine (^{18}F -FLT), 1-(2'-deoxy-2'-[^{18}F]fluoro- β -D-arabinofuranosyl) thymidine (^{18}F -FMAU), and 1-(2'-deoxy-2'-[^{18}F]fluoro- β -D-arabinofuranosyl) uracil (^{18}F -FAU) in patients with advanced cancer.

Methods: Fifteen patients were imaged, five with each imaging agent. Patients had been previously diagnosed with breast, colorectal, gastric, and esophageal cancers and had not received therapy for at least 4 weeks prior to the first scan, and had not been treated with any prior fluoropyrimidines. Subjects were imaged within a week before the start of capecitabine and on the second day of treatment, after the third dose of capecitabine. Tracer uptake was quantified by mean standard uptake value (SUV_{mean}) and using kinetic analysis.

Results: Patients imaged with ^{18}F -FLT showed variable changes in retention and two patients exhibited an increase in SUV_{mean} of 172.3 and 89.9 %, while the other patients had changes ranging from +19.4 to -25.4 %. The average change in ^{18}F -FMAU retention was 0.2 % (range -24.4 to 23.1) and ^{18}F -FAU was -10.2 % (range -40.3 to 19.2). Observed changes correlated strongly with SUV_{max} but not kinetic measurements.

Conclusions: This pilot study demonstrates that patients treated with capecitabine can produce a marked increase in ^{18}F -FLT retention in some patients, which will require further study to determine if this flare is predictive of therapeutic response. ^{18}F -FAU and ^{18}F -FMAU showed little change, on average, after treatment.

Keywords: PET, Oncology, Capecitabine, FLT, FMAU, FAU

Background

Capecitabine is a carbamate prodrug form of 5-fluorouracil (5-FU), approved for the treatment of metastatic colorectal and breast cancers, and can be used as monotherapy or in combination with other cytotoxic and targeted agents [1, 2]. Conversion to 5-FU is accomplished via the action of three enzymes:

carboxylesterase, cytidine deaminase, and thymidine phosphorylase, the latter of which is found at higher concentrations in tumor cells than in normal tissue [3, 4]. Following conversion to 5-FU, anti-tumor activity is achieved via inhibition of thymidylate synthase (TS) and incorporation of 5-FU into RNA and DNA [4, 5]. Despite its widespread use, additional research is needed to explore its mechanisms of cytotoxicity, activation, metabolism, and to develop methods to monitor efficacy.

Due to its effects on thymidine synthesis and incorporation pathways, capecitabine may alter the uptake and

* Correspondence: shieldsa@karmanos.org

²Karmanos Cancer Institute and Oncology, Wayne State University, 4100 John R., HW04HO, Detroit, MI 48201, USA

Full list of author information is available at the end of the article

retention of thymidine analogs used with positron emission tomography (PET) imaging and this could provide a method for assessing response and understanding drug pharmacodynamics. In part, this is due to increased expression of thymidine kinase 1 (TK1) in the salvage pathway, which is involved in the uptake and utilization of thymidine from the plasma through phosphorylation. Increased TK1 expression in tumors has been imaged with ^{11}C -thymidine and thymidine analogs such as 3'-deoxy-3'-[^{18}F]fluorothymidine (^{18}F -FLT) [6–8]. ^{18}F -FLT has been used to monitor cell proliferation [9, 10], since after uptake by tumor nucleoside transporters, ^{18}F -FLT is phosphorylated by TK1, causing it to be trapped intracellularly [11, 12]. Because ^{18}F -FLT is unable to incorporate into the DNA structure due to the lack of a 3' hydroxyl, its retention principally reflects intracellular TK1 activity [13–15]. Uptake of FLT is reproducible and has been shown to be correlated with the proliferative marker Ki-67 [6, 10, 16].

1-(2'-deoxy-2'-fluoro- β -D-arabinofuranosyl) thymidine (FMAU) is another thymidine analogue that was originally introduced as an anti-viral and anti-neoplastic compound, but was later abandoned due to severe toxicity [17, 18]. More recently, FMAU has been adapted to molecular imaging [6, 19]. A key difference between FMAU and FLT is that FMAU has an intact 3' hydroxyl group and can therefore incorporate into the DNA [20]. Furthermore, FMAU is a more potent substrate for thymidine kinase 2 (TK2), located in the mitochondria, than TK1 [18]. Unlike TK1, TK2 is constitutively expressed, with low activity in both dividing and quiescent cells [21, 22]. Accumulation of ^{18}F -FMAU is higher in tumors than most healthy tissues and preclinical studies have shown that its uptake is enhanced in response to conditions that produce an increase in mitochondrial mass such as oxidative, reductive, and energy stress [23, 24]. In addition, low physiologic uptake of ^{18}F -FMAU by normal bone marrow may allow it to be useful in the detection and monitoring of bone marrow metastases [19]. Further, the rapid clearance of ^{18}F -FMAU from the blood in humans (90 % cleared within 10 min), allows for improved imaging in the pelvis compared to ^{18}F -FLT and shortened imaging time [19, 25].

1-(2'-deoxy-2'-fluoro- β -D-arabinofuranosyl) uracil (FAU) is a nucleoside analog that functions as a prodrug form of FMAU [20]. Following cellular uptake of FAU, it is phosphorylated to FAU monophosphate (FAU-MP) and then converted to FMAU monophosphate (FMAU-MP) via the action of TK1 and TS, respectively [26]. FMAU-MP is then incorporated into DNA, resulting in cell death [27]. Dependence on TS for activation was designed to target FAU against malignancies with high expression of this enzyme and to avoid the neurotoxicity that resulted in the discontinuation of clinical FMAU use [17, 28–30]. High

expression of TS is a major mechanism of resistance to chemotherapeutic agents such as 5-FU and capecitabine and has been associated with poor clinical outcome in breast and colorectal cancer [31–33]. Furthermore, the structure of FAU allows for its tissue distribution to be monitored using PET, and potentially serve as a technique for imaging the *de novo* TdR synthesis pathway [34, 35]. To that end, studies of ^{18}F -FAU in humans and dogs found have found higher uptake in tumors than normal tissue [28, 29]. More recently, a pharmacokinetic modeling study demonstrated that the conversion of FAU to FMAU is greatly increased in tumors compared to normal tissues [36]. Although its clinical use was discontinued due to hepatotoxicity, FAU may have some utility as an imaging agent.

The purpose of this study was to monitor the retention of radiolabeled fluoropyrimidines: ^{18}F -FLT, ^{18}F -FMAU, and ^{18}F -FAU in patients with breast and gastrointestinal cancers who received capecitabine. Given the differences in metabolism for each of the tracers, the effects of capecitabine were expected to vary. The primary objective was to monitor changes in tracer uptake as measured by mean standardized uptake value (SUV_{mean}) along with kinetic parameters. These parameters may provide an approximation of the physiological effect of capecitabine on tumors.

Methods

Radiochemistry and patient imaging

PET tracers were synthesized as previously published and patients were injected intravenously with ^{18}F -FLT (range, 347–389 MBq; mean 372 MBq), ^{18}F -FAU (range, 211–396 MBq; mean 346 MBq), or ^{18}F -FMAU (range, 191–388 MBq; mean 339 MBq) over 60s as described [25, 37, 38]. Subjects underwent dynamic PET with a series of timed images (4×20s, 4×40s, 4×60s, and 4×180s). In patients injected with ^{18}F -FLT and ^{18}F -FAU, but not ^{18}F -FMAU, an additional series of images was collected (8×300s). PET was conducted with a 15-cm field of view over the area of the tumors (neck, thorax, or abdomen) followed by a whole body image using an Exact/HR tomograph (Siemens Medical Solutions, Malvern, Pennsylvania, USA).

Fifteen patients with solid tumors were imaged, five with each of the fluorine-18 labeled PET tracers. Patient accrual alternated between the three agents based primarily on tracer availability. Malignancies included were breast, colorectal, gastric, and esophageal cancers (Table 1; Additional file 1: Table S1). Patients had not received therapy for at least 4 weeks prior to the first PET scan, and had not been previously treated with 5-FU, capecitabine or other fluoropyrimidines. Six of the 15 patients studied received capecitabine alone. Other patients were placed on standard regimens, which utilized

radiotherapy and oxaliplatin as well as targeted agents such as lapatinib, bevacizumab, and trastuzumab (Table 1). When capecitabine was combined with other treatments they were started after the third dose of capecitabine and after completion of the final PET scan. Patients underwent imaging within one week before therapy, and again one day after the start of therapy, after receiving three doses of capecitabine. The mean time between scans was 3.7 days (range 2–7 days).

Patient images were analyzed with PMOD (Zurich, Switzerland) software and regions of interest (ROIs) were defined in a semi-automated fashion as published [19]. ROIs were chosen in the three adjacent planes with the highest activity, using isocontours halfway between the minimum and maximum thresholds of the tumor. Tracer uptake was measured by standardized uptake value (SUV). Mean SUVs (SUV_{mean}) were calculated on whole ROIs, and maximum SUVs (SUV_{max}) were measured as the pixels with the most activity in the same ROIs.

Kinetic analysis

Kinetic modeling was conducted using PMOD (Zurich, Switzerland) software as has been published previously [39]. In short, ^{18}F -FLT and ^{18}F -FAU time-activity curves were fitted using a 3-compartment model, which produced rate constants K_1 , k_2 , and k_3 . K_1 (mL/g/min) represents the unidirectional transport of tracer from blood into tissue, k_2 (min^{-1}) represents the reverse transport, and k_3 (min^{-1}) characterizes phosphorylation and intracellular trapping via thymidine kinase-1 activity. The flux values for ^{18}F -FLT and ^{18}F -FAU were then calculated as $K_1 \times k_3 / (k_2 + k_3)$. Tumor uptake values and

blood tissue kinetics were interpreted with respect to the blood activity level, obtained from measurements of tracer activity within great vessels.

For ^{18}F -FMAU kinetic analysis, we utilized tumor retention ratio (TRR), which has been shown to correlate strongly with compartmental-K. TRR was obtained by dividing the tumor ^{18}F -FMAU activity—obtained in an image from 5 to 11 min post-injection—area under the curve (AUC) by of ^{18}F -FMAU blood activity AUC. AUC values were calculated using GraphPad Prism version 6 (GraphPad Software, La Jolla, California, USA), which measures AUC using the trapezoid method. To reduce image noise, the first 5 min were omitted. Furthermore, we have previously shown that in ^{18}F -FMAU blood activity decreases sharply in the first 11 min after injection, and that images taken within the 5–11 window are comparable to images from 50–60 min [19].

Statistical considerations

The relationship of one PET parameter to another was measured using linear regression models, and the goodness of fit of these models was assessed using the r^2 value. Regression models were fit and assessed using GraphPad Prism version 6 (GraphPad Software, La Jolla, California, USA).

Results

^{18}F -FLT PET imaging

Five patients (median age: 62) with breast, esophageal, and colorectal carcinomas were imaged with ^{18}F -FLT at baseline, and then following capecitabine therapy. In addition to capecitabine, 4/5 patients underwent other anti-neoplastic therapy including: oxaliplatin, irinotecan,

Table 1 Clinical patient characteristics

Patient no.	Age	Sex	Tumor type	Other therapy with initial capecitabine	Imaging tracer
1	47	F	Breast	Lapatinib	^{18}F -FLT
2	65	F	Breast	None	
3	62	F	Esophageal	Radiation	
4	62	F	Colorectal	Bevacizumab, Oxaliplatin	
5	56	F	Colorectal	Oxaliplatin	
6	63	F	Breast	None	
7	52	F	Breast	Lapatinib	
8	46	F	Breast	Lapatinib	
9	73	F	Breast	None	
10	63	F	Breast	None	
11	64	F	Breast	None	^{18}F -FAU
12	62	F	Colorectal	Oxaliplatin, Bevacizumab	
13	53	F	Gastric	None	
14	49	M	Colorectal	Radiation	
15	37	M	Esophageal	Oxaliplatin, Trastuzumab	

bevacizumab, lapatinib, and radiation after the second scan (Table 1). Variable changes in tumor activity were observed post-treatment (Table 2; Additional file 2: Table S2). Patient 3 exhibited the largest change in SUV_{mean} , with an increase of 172.3 % from baseline (Fig. 1). Patient 4 also had a marked change in tracer retention, with an increase in SUV_{mean} of 89.9 % after capecitabine. The other three patients imaged had more modest changes in tumor SUV_{mean} , ranging from an increase of 19.4 % to a decline of 25.4 %. Although the primary endpoint was tracer uptake as measured by SUV_{mean} , the changes observed correlated with changes in SUV_{max} ($r^2 = 0.98$, $P = 0.0014$). Although differences in tracer flux, calculated from compartmental-K, trended with changes in tumor SUV (Table 2), changes in flux and SUV_{mean} were not correlated ($r^2 = 0.57$, $P = 0.1404$).

^{18}F -FMAU PET imaging

Five patients with breast cancer (median age: 63) were imaged with ^{18}F -FMAU at baseline and following capecitabine treatment. Two patients received lapatinib after the start of capecitabine (Table 1). Although tumor activity was consistently high in patients imaged with ^{18}F -FMAU (median SUV_{mean} at baseline: 2.58), there was non-specific tracer uptake throughout the lungs, which gave images a 'grainy' appearance (Fig. 2). Following capecitabine treatment, SUV_{mean} values ranged from an increase in 23.1 % to a decline of 24.4 % from baseline, with an average change of 0.2 % (Table 3; Additional file 2: Table S2). SUV_{mean} correlated strongly with SUV_{max} measurements ($r^2 = 0.95$, $P = 0.005$). As mentioned, TRR was used for kinetic analysis in lieu of compartmental-K in patients imaged with ^{18}F -FMAU because the rapid clearance of FMAU prevents the establishment of equilibrium between tissue compartments [19]. Similarly to what was observed in patients imaged with ^{18}F -FLT, differences in SUV_{mean} and TRR after treatment trended in the same direction, but were not strongly correlated ($r^2 = 0.65$, $P = 0.098$).

^{18}F -FAU PET imaging

Five patients (median age: 53) with breast, gastric, colorectal, and esophageal junction tumors underwent ^{18}F -FAU PET scans at baseline and after capecitabine treatment. Two patients received capecitabine alone, and the

remaining three also received treatment with either an antibody or radiation (Table 1). The majority of the patients showed little change in tracer uptake post-treatment (average change -10.2 %) (Table 4, Additional file 2: Table S2). Only patient 15 displayed a notable change in ^{18}F -FAU retention, with a decline of 40.3 % after capecitabine (Fig. 3). Like the previous tracers, ^{18}F -FAU retention was high in the kidneys and liver, but greater non-specific tissue uptake was observed compared to patients imaged with ^{18}F -FLT and ^{18}F -FMAU. In addition, of the tracers studied, ^{18}F -FAU had the lowest tumor activity. As with ^{18}F -FLT, changes in SUV_{mean} measurements correlated strongly with changes in SUV_{max} ($r^2 = 0.98$, $P = 0.001$). Tracer flux was calculated for 4/5 patients, with patient 11 being unevaluable due to lack of dynamic imaging. As with the previous two tracers studied herein, in patients imaged with ^{18}F -FAU, tracer flux and SUV_{mean} were not significantly correlated ($r^2 = 0.72$, $P = 0.1534$). Furthermore, mean pretreatment ^{18}F -FAU flux values were far lower than what was observed with ^{18}F -FLT (0.0059 cc/min versus 0.0251 cc/min), further underscoring the low tumor accumulation of ^{18}F -FAU in this patient cohort.

Discussion

Although several radiolabeled molecules have been developed for use with PET, 2'-deoxy-2'-[^{18}F]fluoro-D-glucose (^{18}F -FDG) remains the principal approved compound for the detection and staging of cancer. Although ^{18}F -FDG uptake correlates with general tumor metabolism, this may not accurately describe the proliferative capacity of cancers, which is a major consideration for treatment and prognosis. Further, because many chemotherapeutics used today function by impairing cellular proliferation, it is desirable to develop imaging modalities to monitor these pathways. Accordingly, we sought to examine the effect of capecitabine, a frequently used anti-neoplastic compound, on the uptake and retention of three nucleoside analogs. The goal of this study was to gain an increased understanding of the effect of capecitabine on tumor thymidine metabolism, and to assess the usefulness of these tracers in the setting of cancer treatment.

Table 2 Tumor retention in patients imaged with ^{18}F -FLT

Patient No.	Tumor SUV_{mean}			Tracer flux into tumor (cc/min)		
	Baseline	Post-treatment	% Change	Baseline	Post-treatment	% Change
1	1.97	1.58	-19.8	0.0271	0.0211	-22.1
2	1.96	2.34	19.4	0.0314	0.0526	67.5
3	4.70	12.80	172.3	0.0217	0.0796	266.8
4	2.27	4.31	89.9	0.0187	0.1090	482.9
5	1.34	1.00	-25.4	0.0267	0.0213	-20.2

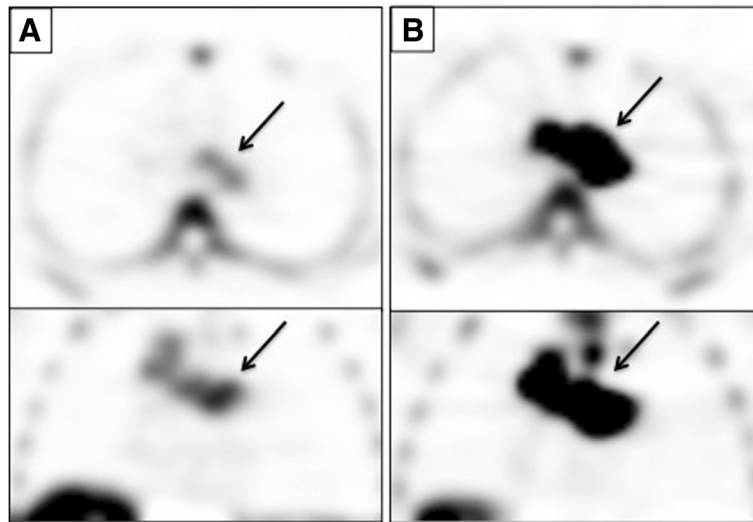


Fig. 1 Tumor ^{18}F -FLT Uptake in Patient 3. Axial (top) and coronal (bottom) ^{18}F -FLT Images of a mediastinal metastasis (arrow) in a patient with esophageal cancer at baseline (a) and after 1 day of capecitabine therapy (b). Tumor SUV_{mean} increased from 4.70 to 12.80

When evaluating changes in PET tracer accumulation, it is important to understand the reproducibility of such measurements in order to distinguish changes in tumor biology from simple scan-to-scan variance. A previous study in 9 non-small cell lung cancer patients found the error of ^{18}F -FLT-PET to be approximately 20 % [16]. More recently, a multi-center trial examining the repeatability of PET with ^{18}F -FDG in untreated patients found tumor SUV to vary between a decrease of 30 % to an increase of 40 % [40]. Although, there have been no studies examining the repeatability of imaging with ^{18}F -FMAU or ^{18}F -FAU, tumor retention of these tracers is

lower than ^{18}F -FDG, and thus, one would not expect improved reproducibility. In our study we do not think that the changes seen between PET scans reflect tumor progression, since the time between baseline and post-treatment scans ranged from 2 to 7 days. Furthermore, we do not think that a response to treatment could cause any clinical decline in the tumor, since the second scan was done a day after the start of therapy with capecitabine.

Patients imaged with ^{18}F -FLT had a variable change in uptake after treatment, with two patients displaying a substantial increase in tumor retention (89.9 and 172.3 %). Since ^{18}F -FLT uptake reflects cellular TK1, the

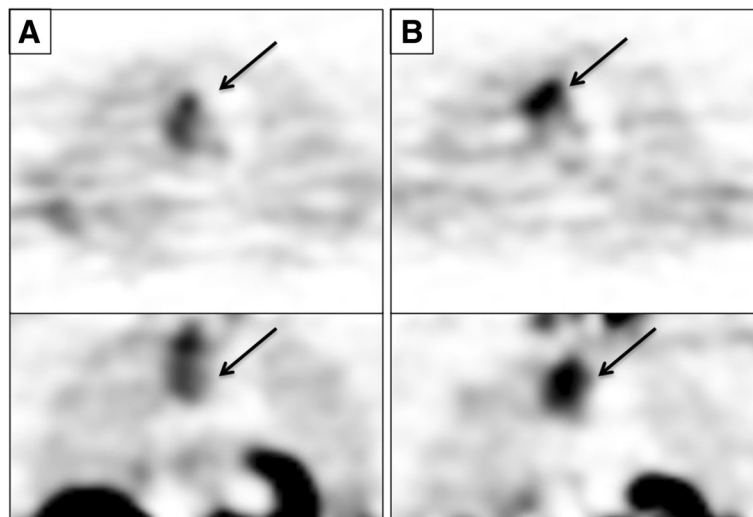


Fig. 2 Tumor ^{18}F -FMAU Uptake in Patient 7. Axial (top) and coronal (bottom) ^{18}F -FMAU Images of a lung metastasis (arrow) in a patient with breast cancer at baseline (a) and after 1 day of capecitabine therapy (b). Tumor SUV_{mean} increased from 3.76 to 4.63

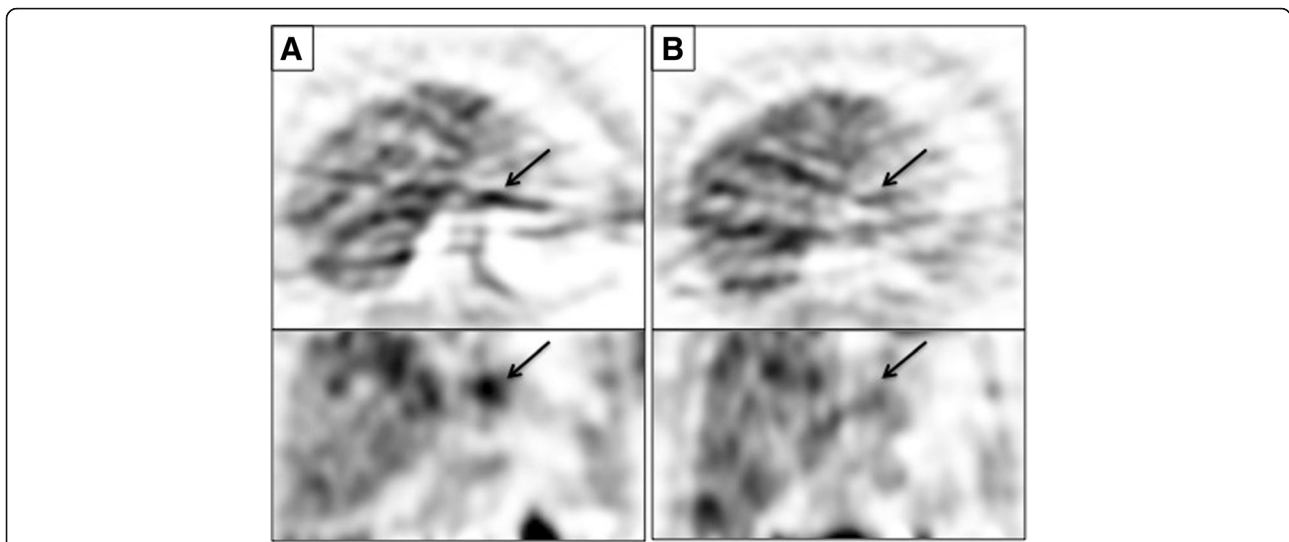


Fig. 3 Tumor ^{18}F -FAU Uptake in Patient 15. Axial (top) and coronal (bottom) ^{18}F -FAU Images of a tumor of the gastroesophageal junction (arrow) at baseline (a) and after 1 day of capecitabine therapy (b). Tumor SUV_{mean} decreased from 3.47 to 2.07

large increase in SUV_{mean} indicates an upregulation of TK1 activity following capecitabine. This may be caused by the inhibitory effect of 5-FU on TS [41]. As thymidine levels drop due to TS inhibition, there is an increase in TK1 activity as cells attempt to replenish thymidine exogenously. This increase leads to a window of 1–24 h in which ^{18}F -FLT uptake is significantly increased, and has been termed the ‘flare’ phenomenon [42, 43]. This effect has been observed in response to nucleoside analogs: 5-FU and gemcitabine, as well as antifolates: methotrexate and pemetrexed in preclinical models of glioma, esophageal, colon, and breast cancer [41–46].

A recent study examining the flare phenomenon in colorectal cancer patients treated with 5-FU and oxaliplatin found that ^{18}F -FLT accumulation increased in all patients 24 h after treatment, but increases in tumor $\text{SUV} > 45.8\%$ were associated with poor treatment outcomes [47]. It is possible that a large flare may suggest that cancers are able to successfully compensate for drug-induced TS inhibition. Therefore, a large increase in ^{18}F -FLT retention may be a negative indicator of therapy response. Conversely, the absence of change in ^{18}F -FLT retention in the remaining three patients may

suggest that patient tumors were unable to effectively adapt to capecitabine treatment. Alternatively, the absence of a flare could be due to upregulation of intracellular TS levels leading to drug resistance, or inefficient conversion of capecitabine to 5-FU [48].

Subjects imaged with ^{18}F -FMAU demonstrated little change in tracer retention after treatment. The average change in tumor SUV_{mean} was 0.18 % (range -24.4 to 23.1) (Table 3). Previous studies have shown increases in ^{18}F -FMAU retention in response to oxidative, reductive, and energy stresses due to upregulation of mitochondrial TK2 levels [49]. Furthermore, it has been shown that anti-cancer agents can lead to an increase in mitochondrial mass during apoptosis [50, 51]. Interestingly, patients imaged with ^{18}F -FMAU had the highest baseline tumor uptake: 2.58 versus 2.45 in patients scanned with ^{18}F -FLT and 1.99 patients scanned with ^{18}F -FAU. These findings suggest that while tumor cells are under a high basal level of cellular stress, this is not increased significantly by short-term capecitabine treatment.

Similar to patients imaged with ^{18}F -FMAU, patients scanned with ^{18}F -FAU demonstrated little change in tracer retention after capecitabine (Table 4), with an average

Table 3 Tumor uptake in patients imaged with ^{18}F -FMAU

Patient no.	Tumor SUV_{mean}			Tumor retention ratio		
	Baseline	Post-treatment	% Change	Baseline	Post-treatment	% Change
6	4.64	5.06	9.1	3.01	3.47	15.3
7	3.76	4.63	23.1	3.56	3.9	9.6
8	1.97	2.11	7.1	2.18	2.74	25.7
9	2.58	1.95	-24.4	2.03	1.65	-18.9
10	2.14	1.84	-14.0	1.22	0.96	-21.3

Table 4 Tumor retention in patients imaged with ^{18}F -FAU

Patient no.	Tumor SUV _{mean}			Tracer flux into tumor (cc/min)		
	Baseline	Post-treatment	% Change	Baseline	Post-Treatment	% Change
11	1.03	1.06	2.9	No Dynamic Images		
12	1.05	0.87	-17.1	0.0032	0.0019	-40.6
13	2.57	2.15	-16.3	0.0058	0.0055	-5.2
14	1.82	2.17	19.2	0.0108	0.0158	46.3
15	3.47	2.07	-40.3	0.0039	0.0029	-25.6

change in SUV_{mean} of -10.2 %. No difference in measurement may be due to several factors, including elevated tumor TS. As discussed, high tumor TS is a common mechanism of treatment resistance in breast and colorectal cancers [33]. In this case TS will continue to convert FAU-P to FMAU-P, with treatment having a negligible effect on this process. One patient demonstrated a decrease of 40.3 % in tumor SUV_{mean} from baseline in response to capecitabine. This may be evidence of inhibition of TS by capecitabine, given that TS required for retention of ^{18}F -FAU [26]. It is worth noting, however, that tumor activity was lowest in patients imaged with ^{18}F -FAU, suggesting a low level of tumor specificity for this tracer.

Major limitations of this study included small sample sizes and heterogenous patient cohorts. Patients enrolled in this study had several different malignancies and received varied treatment regimens (Table 1 and Additional file 1: Table S1). The duration of capecitabine treatment after the second PET scan was inconsistent between individuals and the majority of subjects (9 of 15) were administered other anti-neoplastic therapy in addition to capecitabine. For these reasons, we are unable to correlate our imaging findings to patient response to capecitabine and therefore our results should be considered observational.

Conclusions

In this exploratory study, we sought to monitor the response of patient tumors to capecitabine, a commonly used chemotherapeutic, using three experimental imaging tracers: ^{18}F -FLT, ^{18}F -FMAU, and ^{18}F -FAU. Patients who underwent PET with ^{18}F -FAU and ^{18}F -FMAU showed little change, on average, after treatment. However, in-line with similar studies, we observed that patients treated with capecitabine can produce a marked increase in ^{18}F -FLT retention in some patients. Further studies are warranted to determine if this effect could be used as an early biomarker for therapeutic efficacy.

Additional files

Additional file 1: Table S1. Additional Patient Information. (XLSX 10 kb)

Additional file 2: Table S2. Patient Image Data. (XLSX 19 kb)

Abbreviations

5-FU: 5-Fluorouracil; AUC: Area under the curve; FAU: 1-(2'-deoxy-2'-fluoro-β-D-arabinofuranosyl) Uracil; FAU-P: FAU Monophosphate; FDG: 2'-deoxy-2'-fluoro-D-glucose; FLT: 3'-deoxy-3'-fluorothymidine; FMAU: 1-(2'-deoxy-2'-fluoro-β-D-arabinofuranosyl) Thymidine; FMAU-P: FMAU Monophosphate; PET: Positron emission tomography; ROI: Region of interest; SUV: Standardized uptake value; TK1: Thymidine kinase 1; TRR: Tumor retention ratio; TS: Thymidylate synthase

Acknowledgements

The authors would like to acknowledge Janice Akoury for her guidance in the revision of this manuscript.

Funding

The work was funded in part by contract 26XS295 from the National Cancer Institute.

Availability of data and material

A spreadsheet containing additional patient data has been submitted alongside this manuscript.

Authors' contributions

Manuscript was drafted by CM and AS; AS and JC were responsible for study design and conception; CM, JLC, SJ were responsible for data analysis; KD aided in data collection; DM was responsible for patient follow-up; TM synthesized radiotracers. All authors read and approved the final manuscript.

Authors' information

Not Applicable.

Competing interests

J.M. Collins is a co-inventor for patents related to portions of this work, which have been assigned to the U.S. government. The remaining authors declare that they have no competing interest.

Consent for publication

Not Applicable.

Ethics approval and consent to participate

The human subject protocol for this study was reviewed and approved by the Human Investigation Committee of Wayne State University and the Radioactive Drug Research Committee. All patients signed a written informed consent prior to enrollment into the study.

Author details

¹Cancer Biology Graduate Program, Wayne State University, Detroit, MI 48201, USA. ²Karmanos Cancer Institute and Oncology, Wayne State University, 4100 John R., HW04HO, Detroit, MI 48201, USA. ³Radiology, Wayne State University, Detroit, MI 48201, USA. ⁴National Cancer Institute, Bethesda, MD 20892, USA.

Received: 21 June 2016 Accepted: 3 October 2016

Published online: 17 October 2016

References

- Koukourakis GV, Kouloulis V, Koukourakis MJ, Zacharias GA, Zabatis H, Kouvaris J. Efficacy of the oral fluorouracil pro-drug capecitabine in cancer treatment: a review. *Molecules*. 2008;13:1897–922.

2. Simplicio AL, Clancy JM, Gilmer JF. Prodrugs for amines. *Molecules*. 2008;13:519–47.
3. Budman DR, Meropol NJ, Reigner B, Creaven PJ, Lichtman SM, Berghorn E, Behr J, Gordon RJ, Osterwalder B, Griffin T. Preliminary studies of a novel oral fluoropyrimidine carbamate: capecitabine. *J Clin Oncol*. 1998;16:1795–802.
4. Miwa M, Ura M, Nishida M, Sawada N, Ishikawa T, Mori K, Shimma N, Umeda I, Ishitsuka H. Design of a novel oral fluoropyrimidine carbamate, capecitabine, which generates 5-fluorouracil selectively in tumours by enzymes concentrated in human liver and cancer tissue. *Eur J Cancer*. 1998;34:1274–81.
5. Schuetz JD, Wallace HJ, Diasio RB. 5-Fluorouracil incorporation into DNA of CF-1 mouse bone marrow cells as a possible mechanism of toxicity. *Cancer Res*. 1984;44:1358–63.
6. Tehrani OS, Shields AF. PET imaging of proliferation with pyrimidines. *J Nucl Med*. 2013;54:903–12.
7. Barthel H, Perumal M, Latigo J, He Q, Brady F, Luthra SK, Price PM, Aboagye EO. The uptake of 3'-deoxy-3'-[18 F]fluorothymidine into L5178Y tumours in vivo is dependent on thymidine kinase 1 protein levels. *Eur J Nucl Med Mol Imaging*. 2005;32:257–63.
8. Soloviev D, Lewis D, Honess D, Aboagye E. [(18)F]FLT: an imaging biomarker of tumour proliferation for assessment of tumour response to treatment. *Eur J Cancer*. 2012;48:416–24.
9. Buck AK, Schirmeister H, Hetzel M, Von Der Heide M, Halter G, Glatting G, Mattfeldt T, Liewald F, Reske SN, Neumaier B. 3-deoxy-3'-[(18)F]fluorothymidine-positron emission tomography for noninvasive assessment of proliferation in pulmonary nodules. *Cancer Res*. 2002;62:3331–4.
10. Chalkidou A, Landau DB, Odell EW, Cornelius VR, O'Doherty MJ, Marsden PK. Correlation between Ki-67 immunohistochemistry and 18 F-fluorothymidine uptake in patients with cancer: A systematic review and meta-analysis. *Eur J Cancer*. 2012;48:3499–513.
11. Kong XB, Zhu QY, Vidal PM, Watanabe KA, Polsky B, Armstrong D, Ostrand M, Lang Jr SA, Muchmore E, Chou TC. Comparisons of anti-human immunodeficiency virus activities, cellular transport, and plasma and intracellular pharmacokinetics of 3'-fluoro-3'-deoxythymidine and 3'-azido-3'-deoxythymidine. *Antimicrob Agents Chemother*. 1992;36:808–18.
12. Shields AF, Grierson JR, Dohmen BM, Machulla HJ, Stayanoff JC, Lawhorn-Crews JM, Obradovich JE, Muzik O, Mangner TJ. Imaging proliferation in vivo with [F-18]FLT and positron emission tomography. *Nat Med*. 1998;4:1334–6.
13. Grierson JR, Schwartz JL, Muzi M, Jordan R, Krohn KA. Metabolism of 3'-deoxy-3'-[F-18]fluorothymidine in proliferating A549 cells: validations for positron emission tomography. *Nucl Med Biol*. 2004;31:829–37.
14. Rasey JS, Grierson JR, Wiens LW, Kolb PD, Schwartz JL. Validation of FLT uptake as a measure of thymidine kinase-1 activity in A549 carcinoma cells. *J Nucl Med*. 2002;43:1210–7.
15. Schwartz JL, Tamura Y, Jordan R, Grierson JR, Krohn KA. Monitoring tumor cell proliferation by targeting DNA synthetic processes with thymidine and thymidine analogs. *J Nucl Med*. 2003;44:2027–32.
16. Shields AF, Lawhorn-Crews JM, Briston DA, Zalzal S, Gadgeel S, Douglas KA, Mangner TJ, Heilbrun LK, Muzik O. Analysis and reproducibility of 3'-Deoxy-3'-[18 F]fluorothymidine positron emission tomography imaging in patients with non-small cell lung cancer. *Clin Cancer Res*. 2008;14:4463–8.
17. Abbruzzese JL, Schmidt S, Raber MN, Levy JK, Castellanos AM, Legha SS, Krakoff IH. Phase I trial of 1-(2'-deoxy-2'-fluoro-1-beta-D-arabinofuranosyl)-5-methyluracil (FMAU) terminated by severe neurologic toxicity. *Invest New Drugs*. 1989;7:195–201.
18. Bading JR, Shahinian AH, Vail A, Bathija P, Koszalka GW, Koda RT, Alauddin MM, Fissekis JD, Conti PS. Pharmacokinetics of the thymidine analog 2'-fluoro-5-methyl-1-beta-D-arabinofuranosyluracil (FMAU) in tumor-bearing rats. *Nucl Med Biol*. 2004;31:407–18.
19. Tehrani OS, Muzik O, Heilbrun LK, Douglas KA, Lawhorn-Crews JM, Sun H, Mangner TJ, Shields AF. Tumor imaging using 1-(2'-deoxy-2'-18 F-fluoro-beta-D-arabinofuranosyl)thymine and PET. *J Nucl Med*. 2007;48:1436–41.
20. Collins JM, Klecker RW, Katki AG. Suicide prodrugs activated by thymidylate synthase: rationale for treatment and noninvasive imaging of tumors with deoxyuridine analogues. *Clin Cancer Res*. 1999;5:1976–81.
21. Munch-Petersen B, Thyrdst G. Induction of thymidine kinases in phytohaemagglutinin-stimulated human lymphocytes. *Biochim Biophys Acta*. 1977;478:364–75.
22. Amer ES, Spasokoukotskaja T, Eriksson S. Selective assays for thymidine kinase 1 and 2 and deoxycytidine kinase and their activities in extracts from human cells and tissues. *Biochem Biophys Res Commun*. 1992;188:712–8.
23. Berk AJ, Meyer BJ, Clayton DA. Mitochondrial-specific thymidine kinase. *Arch Biochem Biophys*. 1973;154:563–5.
24. Koch J, Storstad EL. Incorporation of [3H]thymidine into nuclear and mitochondrial DNA in synchronized mammalian cells. *Eur J Biochem*. 1967;3:1–6.
25. Sun H, Sloan A, Mangner TJ, Vaishampayan U, Muzik O, Collins JM, Douglas K, Shields AF. Imaging DNA synthesis with [18 F]FMAU and positron emission tomography in patients with cancer. *Eur J Nucl Med Mol Imaging*. 2005;32:15–22.
26. Eiseman JL, Brown-Proctor C, Kinahan PE, Collins JM, Anderson LW, Joseph E, Hamburger DR, Pan SS, Mathis CA, Egorin MJ, Klecker RW. Distribution of 1-(2'-deoxy-2'-fluoro-beta-D-arabinofuranosyl) uracil in mice bearing colorectal cancer xenografts: rationale for therapeutic use and as a positron emission tomography probe for thymidylate synthase. *Clin Cancer Res*. 2004;10:6669–76.
27. Klecker RW, Katki AG, Collins JM. Toxicity, metabolism, DNA incorporation with lack of repair, and lactate production for 1-(2'-fluoro-2'-deoxy-beta-D-arabinofuranosyl)-5-iodouracil in U-937 and MOLT-4 cells. *Mol Pharmacol*. 1994;46:1204–9.
28. Sun H, Collins JM, Mangner TJ, Muzik O, Shields AF. Imaging [18 F]FAU [1-(2'-deoxy-2'-fluoro-beta-D-arabinofuranosyl) uracil] in dogs. *Nucl Med Biol*. 2003;30:25–30.
29. Sun H, Collins JM, Mangner TJ, Muzik O, Shields AF. Imaging the pharmacokinetics of [F-18]FAU in patients with tumors: PET studies. *Cancer Chemother Pharmacol*. 2006;57:343–8.
30. Wang H, Oliver P, Nan L, Wang S, Wang Z, Rhie JK, Zhang R, Hill DL. Radiolabeled 2'-fluorodeoxyuracil-beta-D-arabinofuranoside (FAU) and 2'-fluoro-5-methyldeoxyuracil-beta -D-arabinofuranoside (FMAU) as tumor-imaging agents in mice. *Cancer Chemother Pharmacol*. 2002;49:419–24.
31. Allegra CJ, Paik S, Colangelo LH, Parr AL, Kirsch I, Kim G, Klein P, Johnston PG, Wolmark N, Wieand HS. Prognostic value of thymidylate synthase, Ki-67, and p53 in patients with Dukes' B and C colon cancer: a National Cancer Institute-National Surgical Adjuvant Breast and Bowel Project collaborative study. *J Clin Oncol*. 2003;21:241–50.
32. Aschele C, Lonardi S, Monfardini S. Thymidylate Synthase expression as a predictor of clinical response to fluoropyrimidine-based chemotherapy in advanced colorectal cancer. *Cancer Treat Rev*. 2002;28:27–47.
33. Ichikawa W, Uetake H, Shirota Y, Yamada H, Nishi N, Nihei Z, Sugihara K, Hirayama R. Combination of dihydropyrimidine dehydrogenase and thymidylate synthase gene expressions in primary tumors as predictive parameters for the efficacy of fluoropyrimidine-based chemotherapy for metastatic colorectal cancer. *Clin Cancer Res*. 2003;9:786–91.
34. Johnston PG, Fisher ER, Rockette HE, Fisher B, Wolmark N, Drake JC, Chabner BA, Allegra CJ. The role of thymidylate synthase expression in prognosis and outcome of adjuvant chemotherapy in patients with rectal cancer. *J Clin Oncol*. 1994;12:2640–7.
35. Popat S, Matakidou A, Houlston RS. Thymidylate synthase expression and prognosis in colorectal cancer: a systematic review and meta-analysis. *J Clin Oncol*. 2004;22:529–36.
36. Li J, Kim S, Shields AF, Douglas KA, McHugh CI, Lawhorn-Crews JM, Wu J, Mangner TJ, LoRusso PM. Integrating Dynamic Positron Emission Tomography and Conventional Pharmacokinetic Studies to Delineate Plasma and Tumor Pharmacokinetics of FAU, a Prodrug Bioactivated by Thymidylate Synthase. *J Clin Pharmacol*. 2016;56:1433–47.
37. Mangner TJ, Klecker RW, Anderson L, Shields AF. Synthesis of 2'-deoxy-2'-[18 F]fluoro-beta-D-arabinofuranosyl nucleosides, [18 F]FAU, [18 F]FMAU, [18 F]FBAU and [18 F]FAIU, as potential PET agents for imaging cellular proliferation. Synthesis of [18 F]labelled FAU, FMAU, FBAU, FAIU. *Nucl Med Biol*. 2003;30:215–24.
38. Shields AF, Grierson JR, Muzik O, Stayanoff JC, Lawhorn-Crews JM, Obradovich JE, Mangner TJ. Kinetics of 3'-deoxy-3'-[F-18]fluorothymidine uptake and retention in dogs. *Mol Imaging Biol*. 2002;4:83–9.
39. Shields AF, Briston DA, Chandupatla S, Douglas KA, Lawhorn-Crews J, Collins JM, Mangner TJ, Heilbrun LK, Muzik O. A simplified analysis of [18 F]3'-deoxy-3'-fluorothymidine metabolism and retention. *Eur J Nucl Med Mol Imaging*. 2005;32:1269–75.
40. Weber WA, Gatsonis CA, Mozley PD, Hanna LG, Shields AF, Aberle DR, Govindan R, Torigian DA, Karp JS, Yu JQ, et al. Repeatability of 18 F-FDG PET/CT in Advanced Non-Small Cell Lung Cancer: Prospective Assessment in 2 Multicenter Trials. *J Nucl Med*. 2015;56:1137–43.

41. Lee SJ, Kim SY, Chung JH, Oh SJ, Ryu JS, Hong YS, Kim TW, Moon DH. Induction of thymidine kinase 1 after 5-fluorouracil as a mechanism for 3'-deoxy-3'-[18 F]fluorothymidine flare. *Biochem Pharmacol.* 2010;80:1528–36.
42. Dittmann H, Dohmen BM, Kehlbach R, Bartusek G, Pritzkow M, Sarbia M, Bares R. Early changes in [18 F]FLT uptake after chemotherapy: an experimental study. *Eur J Nucl Med Mol Imaging.* 2002;29:1462–9.
43. Kenny LM, Contractor KB, Stebbing J, Al-Nahhas A, Palmieri C, Shousha S, Coombes RC, Aboagye EO. Altered tissue 3'-deoxy-3'-[18 F]fluorothymidine pharmacokinetics in human breast cancer following capecitabine treatment detected by positron emission tomography. *Clin Cancer Res.* 2009;15:6649–57.
44. van Waarde A, Been LB, Ishiwata K, Dierckx RA, Elsinga PH. Early response of sigma-receptor ligands and metabolic PET tracers to 3 forms of chemotherapy: an in vitro study in glioma cells. *J Nucl Med.* 2006;47:1538–45.
45. Saito Y, Furukawa T, Arano Y, Fujibayashi Y, Saga T. Comparison of semiquantitative fluorescence imaging and PET tracer uptake in mesothelioma models as a monitoring system for growth and therapeutic effects. *Nucl Med Biol.* 2008;35:851–60.
46. Paproski RJ, Young JD, Cass CE. Predicting gemcitabine transport and toxicity in human pancreatic cancer cell lines with the positron emission tomography tracer 3'-deoxy-3'-fluorothymidine. *Biochem Pharmacol.* 2010;79:587–95.
47. Hong YS, Kim HO, Kim KP, Lee JL, Kim HJ, Lee SJ, Lee SJ, Oh SJ, Kim JS, Ryu JS, et al. 3'-Deoxy-3'-18 F-fluorothymidine PET for the early prediction of response to leucovorin, 5-fluorouracil, and oxaliplatin therapy in patients with metastatic colorectal cancer. *J Nucl Med.* 2013;54:1209–16.
48. Lee SJ, Choi YL, Park YH, Kim ST, Cho EY, Ahn JS, Im YH. Thymidylate synthase and thymidine phosphorylase as predictive markers of capecitabine monotherapy in patients with anthracycline- and taxane-pretreated metastatic breast cancer. *Cancer Chemother Pharmacol.* 2011;68:743–51.
49. Tehrani OS, Douglas KA, Lawhorn-Crews JM, Shields AF. Tracking cellular stress with labeled FMAU reflects changes in mitochondrial TK2. *Eur J Nucl Med Mol Imaging.* 2008;35:1480–8.
50. Kluza J, Marchetti P, Gallego MA, Lancel S, Fournier C, Loyens A, Beauvillain JC, Bailly C. Mitochondrial proliferation during apoptosis induced by anticancer agents: effects of doxorubicin and mitoxantrone on cancer and cardiac cells. *Oncogene.* 2004;23:7018–30.
51. Mancini M, Anderson BO, Caldwell E, Sedghinasab M, Paty PB, Hockenbery DM. Mitochondrial proliferation and paradoxical membrane depolarization during terminal differentiation and apoptosis in a human colon carcinoma cell line. *J Cell Biol.* 1997;138:449–69.

Submit your next manuscript to BioMed Central and we will help you at every step:

- We accept pre-submission inquiries
- Our selector tool helps you to find the most relevant journal
- We provide round the clock customer support
- Convenient online submission
- Thorough peer review
- Inclusion in PubMed and all major indexing services
- Maximum visibility for your research

Submit your manuscript at
www.biomedcentral.com/submit

